J Mol Model (2016) 22: 141
DOI 10.1007/s00894-016-3003-3

ORIGINAL PAPER

A DFT study on the role of long range correlation interaction and solvent effects in homochiral and heterochiral cyclic trimerization of imidazole based heterocyclic amino acids

N. V. Suresh Kumar[1]

Received: 15 December 2015 / Accepted: 25 April 2016 / Published online: 25 May 2016

Abstract Using B3LYP and B97D functionals of density functional theory (DFT), homochiral and heterochiral cyclic trimerization of imidazole based heterocyclic amino acids are studied in gas phase and solvent phase, i. e., Acetonitrile. Both the functionals show that formation of homochiral cyclic tripeptide is thermodynamically and kinetically favorable over its heterochiral counterpart in gas phase. The functional, B97D, decreases the height of reaction barriers significantly compared to those predicted by the functional B3LYP. The reaction pathways explored using **PCM** implicit solvent model show reduced kinetic favorability for formation of the homochiral cyclic tripeptide over its heterochiral counterpart. The results are substantiated by structural aspects.

Keywords DFT · Cyclic tripeptide · Chirality · Reactivity · long range correlation

Introduction

The present work is an application of density functional theory (DFT) [1] for investigation of cyclic trimerization involving imidazole based heterocyclic amino acids. Two different density functionals, B3LYP [2] and B97D [3] are used in the work, intended to study the role of long range correlation effects in predicting minimum energy conformations. For molecular systems separated by van der Waals distances, where electronic overlap is fairly large [4], accurate measurement of long range correlation energy improves reliability of results. Grimme et al. [3] and Jurecka et al. [5] have developed dispersion corrected, DFT-D, functionals for better description of the systems where damped dispersion interactions are significant. The functionals also describe contribution of intramolecular dispersion for larger molecules [4]. Several studies on polypeptides show that energy ordering of conformations has become much better after inclusion of the dispersion corrections [6–10]. The functional, B3LYP, includes long range non-covalent interactions (at distances > 5 Å) through Hartree-Fock exchange but remain local in correlation [11]. The functional does not describe the R^{-6} asymptotic distance dependence of the dispersion forces [11]. Zhao et al. have reported that B3LYP functional often provides inaccurate hydrogen bond energies [12]. To include the effect of long range dispersion interactions in energetics of the systems, dispersion corrected functional, B97D, was used, besides the functional, B3LYP, in the current study. The long range correlation interaction estimated by B97D, accounts for improving accuracy in estimation of energy of systems compared to that by the functional, B3LYP.

Our earlier DFT study [13] reported that heterochiral cyclic trimerization of 5-(aminoethyl)-2-furan carboxylic acid is kinetically preferred over its homochiral cyclic trimerization based on results obtained from dispersion corrected functional, M06 [14]. The ability of cyclic tripeptide of chiral furan amino acids to form hydrogen bonding with solvent molecule, N, N, dimethyl formamide (**DMF**), enhances with change of stereochemistry at one of the three chiral amino acids in the cyclic tripeptide [13].

Electronic supplementary material The online version of this article (doi:10.1007/s00894-016-3003-3) contains supplementary material, which is available to authorized users.

✉ N. V. Suresh Kumar
nvskumar123@kluniversity.in

[1] Department of Physics, K L University, Green fields, Vaddeswaram, Guntur 522502, India

Importance of cyclic peptides comes from the facts that they are therapeutically potential molecules, show significant resistance towards both exo and endo proteases, functional fine tuning and remarkable size dependent receptor selectivity [15]. Macrocyclization of peptides is a method of synthesizing cyclic peptide with desired properties [16–18]. Indeed, cyclization of small peptides is difficult as the E-geometry of peptide bond prevents to form ring like structure [19]. Structural features that stabilize a linear tripeptide which is precursor to a cyclic tripeptide determine kinetics of cyclization reaction [20, 21].

With a goal to investigate such properties on cyclic tripeptide of Nitrogen based heterocyclic amino acids, we investigated homochiral versus heterochiral cyclic trimerization of imidazole based heterocyclic amino acids using DFT. The importance of scaffolds with three imidazole rings comes from their receptor affinity towards hydroxybenzes [22]. Haberhauer et al. reported that homochiral cyclic tripeptides (**RRR-Cy/SSS-Cy**) of imidazole based heterocyclic amino acids are good molecular receptors for phloroglucinol [22]. The cyclic peptide was synthesized using pentafluorophenyl diphenylphosphinate (FDPP) and Hünig base in acetonitrile with 60 % yield [22].

The present study of DFT calculations on homochiral (**RRR-Cy**) versus heterochiral cyclic (**RRS-Cy**) trimerization of imidazole based heterocyclic amino acids in gas phase and solvent phase with acetonitrile as the solvent reports that homochiral cyclic tripeptide is thermodynamically favorable over heterochiral cyclic tripeptide. The B97D functional that includes long range correlation interactions reduced the activation energy barriers significantly. Kinetically both the homochiral as well as heterochiral cyclic tripeptides are preferable with marginal difference in free energy of activation in solvent phase. We highlight the role of long range correlation, solvent effects and intramolecular interactions in cyclization reactions.

Methods

Initial geometries of **R-**, **S-** isomers of 5-aminoethyl-3-methyl-2-imidazole carboxylic acid (**AEMIC**) and cyclic tripeptides (both homochiral, **RRR-Cy** and heterochiral, **RRS-Cy**) (See Fig. 1) were generated using Avogadro (Application version 1.0.3) [23]. The methyl groups at C_δ-position (chiral center) is kept in such way that it is at *s*-trans orientation with respect to imidazole ring. The geometries were subjected to optimization in gas phase using B3LYP and B97D functionals; and 6-31G(d,p) [24] basis set in both gas phase as well as solvent phase with Acetonitrile as solvent. Polarizable continuum model (**PCM**) [25] of Self Consistent Reaction Field (SCRF) [26] was used

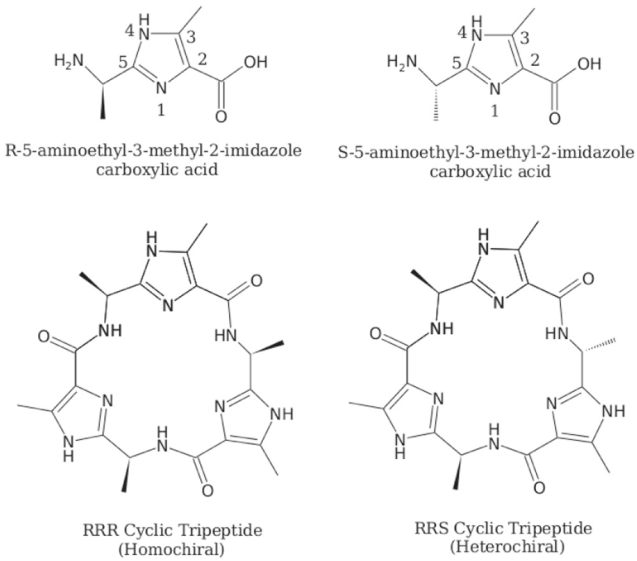

Fig. 1 Schematic representation of **R**, **S-** 5-aminoethyl-3-methyl-2-imidazole carboxylic acids (Monomers), and cyclic tripeptides, **RRR-Cy** (homochiral) and **RRS-Cy** (heterochiral)

to model the solvent phase (Solvent: Acetonitrile). Use of **PCM** is appropriate as it is widely used continuum solvent model and computationally tractable, to predict bulk solvent effects on molecular properties [27]. The model defines a cavity as union of series of interlocking spheres [28]. The electrostatic interactions between solute and solvent including mutual polarization effects are calculated using apparent charge distribution spread over the cavity surface [27]. Effect of non-electrostatic interactions are will be considered in our future work.

Hessian calculations carried out on optimized geometries show real frequencies, indicating that they are at local minimum of their potential energy surface. Thermodynamic properties, free energy, enthalpy and entropy are calculated at temperature of 298.15 K and pressure, 1 atm. Change in zero point vibrational energy corrected electronic energy, (ΔE_z), and free energy, (ΔG), for formation of the cyclic tripeptides were calculated using the following equation.

$$\Delta X = (X_P + 3X_{water}) - 3X_M \quad (1)$$

where X stands for either zero point corrected electronic energy (E_z) or free energy (G). M represents monomer, **AEMIC**, and P stands for cyclic tripeptide.

Reaction pathways

Reaction pathways for cyclization of homochiral (**RRR**) and heterochiral (**RRS**) linear tripeptides were explored using the concerted straight forward peptide bond formation mechanism shown in Fig. 2. Concerted pathway involves direct elimination of water molecule, using the -OH from the carboxyl terminal and -H of amine group [29, 30].

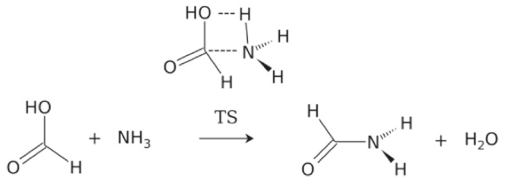

Fig. 2 Uncatalyzed concerted peptide bond formation mechanism suggested in literature

Reaction mechanism for the reverse process, i. e., amide hydrolysis via concerted mechanism is also investigated by Krug et al. [31]. As the straightforward mechanisms offer less computational cost, geometries involved in reaction pathways for the cyclization reactions were modeled using this mechanism in gas phase and solvent phase.

The products are cyclic structures and expected to be conformationally more rigid compared to the reactants and their linear precursors. The number of possible conformers for the linear tripeptides and transition states are relatively larger compared to the cyclic tripeptides. Thus the modeling of the precursor species was based on the minimum energy structures of the products. For example, the transition state, **RRR-TS** was obtained by keeping a water molecule close to the carbonyl group of stable cyclic tripeptide, followed by transition state optimization. The geometries obtained in this process are consistent models for comparing each other.

The optimization and Hessian calculations were carried on the geometries of the pathways using B3LYP/6-31G(d,p) and B97D/6-31G(d,p) levels of theory in both the gas phase as well as solvent phase. Implicit solvent phase model, **PCM**, was used to model the solvent phase, Acetonitrile. The transition states (**TS**) were confirmed by one imaginary frequency and visual analysis of nuclear motion corresponding to the imaginary frequency. Change in free energy (ΔG) of formation of each structure on pathways was calculated to gain insights into thermodynamic and kinetic aspects of cyclization reaction. Also, change in enthalpy (ΔH) and entropic energies (TΔS) corresponding to the change in free energy were estimated.

To verify basis set effect on the results obtained at B3LYP/6-31G(d,p) and B97D/6-31G(d,p) levels of theory, all the geometries explored on the pathway were subjected to single point energy calculations at B3LYP / 6-311++G(2d,2p) // B3LYP / 6-31G(d,p) and B97D / 6-311++G(2d,2p) // B97D/ 6-31G(d,p) levels of theory in both gas phase as well as solvent phase.

Following are the structural parameters used to study the stabilizing interactions in the peptide systems: Hydrogen bond parameters ($\angle$N$\cdots$H-N and distance, N$\cdots$H), Dihedral angle, $\angle$N$\cdots$H-N-C, at C-terminal end of the amino acid and peptide bond length. Magnitude of the dihedral angle provides inferences on planarity of the cyclic tripeptide and stability due to overlapping of the π electrons of conjugated double bonds at the C-terminal end of the amino acids. Resonance in peptide bond results in its partial double bond character and associated stability.

All quantum chemical calculations were carried out using the Gaussian09 [32] suite of programs.

Results and discussion

Coordinates and harmonic vibrations of optimized geometries are shown in Tables, S1 and S2 respectively. Tables S3-S6 show absolute energies of all the species under study. First, free energy of formation of the cyclic tripeptides in gas phase and solvent phase was discussed. Next, the reaction pathways explored in gas phase as well as solvent phase are analyzed to gain kinetic aspects in the formation of the cyclic tripeptides. Finally, structural aspects responsible for cyclic trimerization reactions were presented.

Thermodynamic analysis shows that homochiral cyclic tripeptide is favorable over its heterochiral counterpart

The B3LYP/6-31G(d,p) level of theory predicted that homochiral and heterochiral cyclic tripeptides are favored by 12.0 (12.1) and 11.2 (11.3) kcal/mol in gas phase (solvent phase) respectively (Table 1). The magnitudes of free energy

Table 1 Change in zero point corrected electronic energy (ZPE), ΔE_z, and free energy, ΔG, for formation of cyclic tripeptides at B3LYP/6-31G(d,p) and B97D/6-31G(d,p) levels of theory in gas phase as well as solvent phase, i. e., Acetonitrile (**PCM**)

Functional	Species	Gas Phase		Acetonitrile	
		ΔE_z	ΔG	ΔE_z	ΔG
B3LYP	**RRR-Cy**	−13.2	−12.0	−13.1	−12.1
	RRS-Cy	−12.7	−11.2	−12.5	−11.3
B97D	**RRR-Cy**	−23.3	−21.1	−19.2	−21.5
	RRS-Cy	−18.9	−18.7	−18.8	−19.4

All the values are in kcal/mol

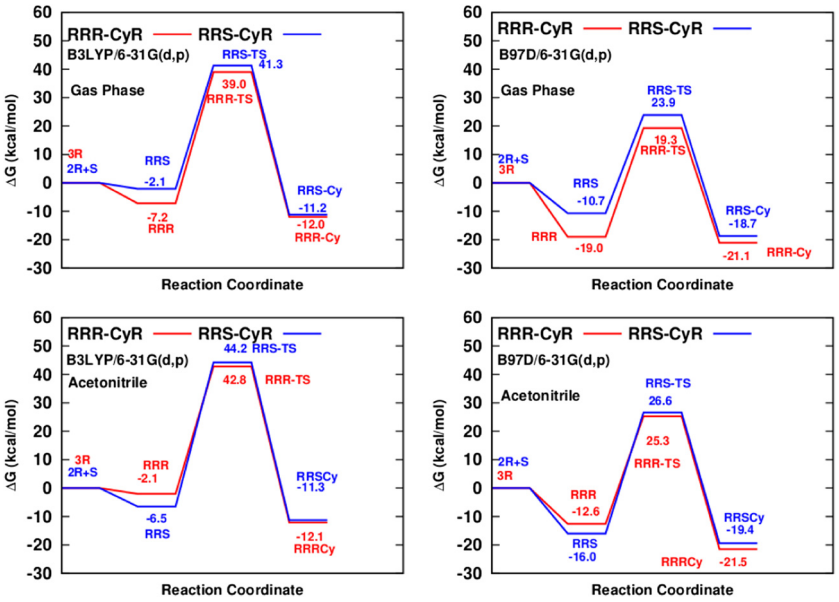

Fig. 3 Information of the cyclization reaction pathway is presented. Relative values of free energy (ΔG) of various structures obtained in pathways of reactions **RRR-CyR** and **RRS-CyR** calculated at B3LYP/6-31G(d,p) and B97D/6-31G(d,p) levels of theory in gas phase as well as Acetonitrile solvent phase modelled using Polarizable Continuum Model

of formation are significantly increased when B97D functional is used instead of B3LYP, i. e, B97D/6-31G(d,p) level of theory predicted that the homochiral and heterochiral cyclic tripeptides are favored by 21.1 (21.5) and 18.7 (19.4) kcal/mol in gas phase (solvent phase) respectively. Both the theories predict that formation of homochiral cyclic tripeptide from 3 units of **R-AEMIC** is slightly favored over formation of heterochiral cyclic tripeptide from 2 units of **R-AEMIC** and 1 unit of **S-AEMIC**.

The trends observed with zero point energy corrected electronic energy remains same as that with free energy data.

Kinetic aspects of cyclic trimerization in solvent phase show reduced preference of homochiral cyclic trimerization over heterochiral cyclic trimerization

Kinetic control in preferential homochiral and heterochiral cyclic trimerization is evaluated by comparing energetics of transition states along concerted reaction pathways shown in Fig. 3. In gas phase, while B3LYP/6-31G(d,p) level of theory predicted free energy of activation for **RRR-TS** (**RRS-TS**) as 39.0 (41.3) kcal/mol, the B97D/6-31G(d,p) level of theory predicted the energy of activation for **RRR-TS** (**RRS-TS**) as 19.3 (23.9) kcal/mol. The B3LYP and B97D functionals preferred homochiral cyclic trimerization with an activation energy difference of 2.3 and 4.6 kcal/mol respectively over heterochiral cyclic trimerization reaction in gas phase. In solvent phase, while B3LYP/6-31G(d,p) level of theory showed the free energy of activation for **RRR-TS** (**RRS-TS**) as 42.8 (44.2) kcal/mol, the B97D/6-31G(d,p) level of theory predicted the energy of activation for **RRR-TS** (**RRS-TS**) as 25.3 (26.6) kcal/mol. The homochiral cyclic trimerization is preferred over heterochiral cyclic trimerization by free energy activation of 1.4 kcal/mol as per B3LYP/6-31G(d,p) level of theory and 1.3 kcal/mol as per B97D/6-31G(d,p) level of theory in solvent phase. Over all, the data show that formation of homochiral cyclic tripeptide is slightly preferred over that of heterochiral cyclic tripeptide in solvent phase compared to that observed in gas phase.

Also, the results indicate the functional, B97D, showed significantly reduced activation energy barriers compared to that obtained from the functional B3LYP. It indicates that long range correlation plays important role in predicting the energies of the species on reaction pathways.

The relative changes of enthalpy (ΔH) and entropic energy (TΔS) of all the geometries on the pathways calculated at B3LYP/6-31G(d,p) and B97D/6-31G(d,p) levels of theory are shown supporting information (Table S7: Gas phase data, Table S8: Solvent phase data). The relative changes of enthalpy follow the trends of free energy data.

Single point energy calculations carried out at B3LYP / 6-311++G(2d,2p) // B3LYP/ 6-31G(d,p) and B97D / 6-311++G(2d,2p) // B97D/ 6-31G(d,p) levels of theory agree with energetic trends discussed above (See Tables S9 and S10).

Linear tripeptides explored in reaction pathways of solvent phase show preferential formation of heterochiral linear tripeptide over homochiral linear tripeptide

The results of gas phase and solvent phase differ significantly in predicting relative magnitudes of free energy (ΔG) for homochiral and heterochiral linear tripeptides. In

gas phase, free energy of formation (ΔG) of homochiral (**RRR**) and heterochiral (**RRS**) linear tripeptides, calculated by B3LYP/6-31G(d,p) (B97D/6-31G(d,p)) level of theory is − 7.2 (− 19.0) and − 2.1 (− 10.7) kcal/mol respectively. Both the theories show that formation of homochiral linear tripeptide is preferred over that of its heterochiral counterpart in gas phase. On the other hand, in solvent phase, heterochiral linear tripeptide is favored over homochiral linear tripeptide by 4.1 kcal/mol ($\Delta G_{RRR} = -2.1$ kcal/mol, $\Delta G_{RRS} = -6.5$ kcal/mol) and 3.4 kcal/mol ($\Delta G_{RRR} = -12.6$ kcal/mol, $\Delta G_{RRS} = -16.0$ kcal/mol) as per B3LYP/6-31G(d,p) and B97D/6-31G(d,p) levels of theory respectively.

The data indicate that preferential formation of heterochiral linear tripeptide over its homochiral counterpart in solvent phase increases the yield of heterochiral cyclic tripeptide compared to that of homochiral cyclic tripeptide.

Geometric analysis substantiates reduced kinetic favorability of homochiral cyclic trimerization over heterochiral cyclization

Monomers optimized at B3LYP/6-31G(d,p) level of theory in gas phase are shown in Fig. S1. Cyclic tripeptides optimized in gas phase and solvent are shown in Figs. 4 and S2 respectively. Also, the geometries of linear tripeptides, and transition states optimized in both the gas phase and solvent phase are shown in Figs. S3–S6 and S7–S10 respectively.

Magnitudes of structural parameters that stabilize all the systems optimized at B3LYP/6-31G(d,p) and B97D/6-31G(d,p) levels of theory, in gas phase, implicit solvent phase (**PCM**) are shown in Tables, S12 and S13 respectively. Related to the linear tripeptides, we are interested in intramolecular H-bond interaction between terminal groups as it plays important role in ring closure mechanism.

B3LYP/6-31G(d,p), Gas phase Both the homochiral and heterochiral cyclic tripeptides are stabilized by weak hydrogen bond interactions (see Table S12 and Fig. 4). The structures of both the cyclic tripeptides have bifurcated N-H···N intramolecular H-bond interactions with N···H distance in the range of 2.26 - 2.33 Å and bond angles in the range of 104.8° - 106.4° in their interior part. Also, the structures show C-H···O intramolecular interactions with O···H distance in the range of 2.32 Å - 2.39 Å and bond angle is about 126.0° in their exterior part. Geometrical parameters of intramolecular hydrogen bond interactions in both the homochiral and heterochiral cyclic peptides are nearly equal in magnitudes.

The dihedral angle at three residues of homochiral cyclic tripeptide is 4.7°. The magnitudes of the angle in heterochiral cyclic tripeptide are −3.4° , 0.6° and 7.2°. The date

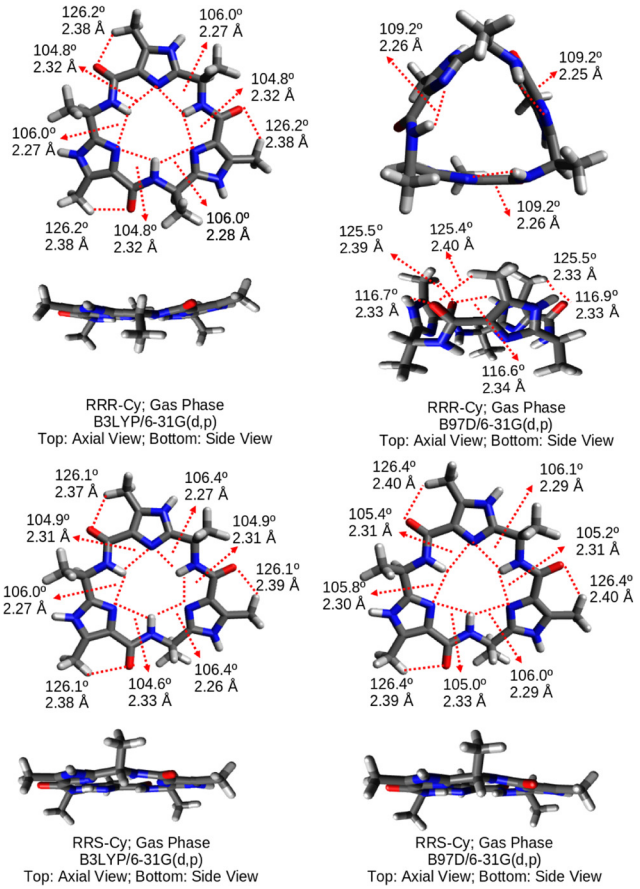

Fig. 4 *Up*: Axial Side views of **RRR** (Homochiral) cyclic tripeptide of **AEMIC**, *Down*: **RRS** (Heterochiral) cyclic tripeptide of **AEMIC** optimized at B3LYP/6-31G(d,p) and B97D/6-31G(d,p) levels of theory in gas phase

indicate that while homochiral cyclic tripeptide is symmetric (C3-Symmetry) and the heterochiral cyclic tripeptide is planar and lacks the symmetry.

The structural parameters of the linear tripeptides, **RRR** and **RRS**, shown in Table S12, supports for N-H···O and O-H···N Hydrogen bonding interaction at its terminals (See Figs. S3 & S4) respectively. The bond angle, ∠N-H···O and distance H···O parameters of H-bond interaction in **RRR** peptide are 159.6° and 2.34 Å. Similarly, the bond angle, ∠O-H···N and distance, H···N in **RRS** are 127.6° and 2.34 Å. Magnitudes of the geometrical parameters support larger stability of homochiral linear tripeptide compared to heterochiral tripeptide shown in energy profile, Fig. 3.

B97D/6-31G(d,p), Gas Phase The homochiral cyclic tripeptide shows significant structural variation compared to that of its heterochiral counterpart. While, in interior part, homochiral cyclic tripeptide show N-H···N hydrogen bond interactions only at C-terminal end of each of the amino acids (N···H distance = 2.26Å, ∠N···H-N = 109.2°),

those at N-terminal end of the amino acid such interaction is not observed. The homochiral cyclic tripeptide is not associated with bifurcated H-bond interactions at its interior part. At exterior part both the cyclic tripeptides, show bifurcated H-bond interactions (C-H$\cdots$O(=C) and N-H$\cdots$O(=C)) are observed (See Fig. 4) with similar magnitudes. The network of H-bond interactions at the interior of heterochiral cyclic tripeptide is similar to that optimized at B3LYP/6-31G(d,p) level of theory, i. e., the H-bond interactions are bifurcated.

The dihedral angle at three residues of homochiral cyclic tripeptide is 11.0°, and magnitudes of the dihedral angles in heterochiral cyclic tripeptide are-3.7°, 0.5° and 6.5°, which indicate that heterochiral cyclic tripeptide is planar compared to that of its homochiral counterpart. The larger dihedral angle of homochiral cyclic tripeptide infers that it shows C3 symmetric bowl shaped structure.

The linear tripeptide, **RRR**, shows N-H$\cdots$O interaction with bond angle, $\angle$N-H$\cdots$O = 159.6° and distance H$\cdots$O = 2.34 Å (See Fig. S5) and **RRS** shows O-H$\cdots$N interaction with $\angle$O-H$\cdots$N = 131.1° and distance H$\cdots$N = 1.99 Å (See Fig. S6). Linearity of the bond supports larger stability of the peptide, **RRR** compared to **RRS** as shown in Fig. 3.

Over all, the structural data analyzed above indicates that change of stereochemistry at one chiral center of the cyclic tripeptide enhances its planarity which causes for bifurcation of intramolecular H-bond interactions. The linear precursor of homochiral cyclic tripeptide is associated with strong H-bond interactions compared to that of heterochiral cyclic tripeptide. The data support homochiral cyclic trimerization.

B3LYP/6-31G(d,p), solvent phase Both the homochiral as well as heterochiral cyclic tripeptides show bifurcated H-bond interactions, N$\cdots$H-N, in the interior part with N$\cdots$H distance in the range of 2.27 - 2.30 Å, the bond angles in the range of 104.8° - 106.2°. The bond length, O$\cdots$H, and bond angle, O$\cdots$H-C of interactions, O$\cdots$H-C, at the exterior part are in the range of 2.42 - 2.45 Å and 124.8 - 125.0°.

The dihedral angle at three residues of homochiral cyclic tripeptide is 3.6° and the values for its counterpart, i. e., heterochiral cyclic tripeptide are −1.2°, −0.7° and 5.3°. The solvent environment also enhanced the planarity of the cyclic tripeptides compared to that of the gas phase structures.

The linear tripeptides, **RRR** shows N-H$\cdots$O interaction with bond angle, $\angle$N-H$\cdots$O = 161.8° and distance H$\cdots$O = 2.49 Å (See Fig. S7) and **RRS** shows O-H$\cdots$N interaction with $\angle$O-H$\cdots$N = 172.1° and distance H$\cdots$N = 1.66 Å (See Fig. S8). Linearity and proximity of the bond supports larger stability of the peptide, **RRS** compared to **RRR** as shown in Fig. 3. This is contrary to the result observed in gas phase.

B97D/6-31G(d,p), solvent phase The structures of homochiral and heterochiral cyclic tripeptide are nearly similar to those optimized at B3LYP/6-31G(d,p) level of theory.

The dihedral angle at three residues of homochiral cyclic tripeptide is 1.6° and the values for its counterpart, i. e., heterochiral cyclic tripeptide are − 0.3°, − 1.7° and 3.0°. The B97D/6-31G(d,p) level of theory increased planarity of the segments, N$\cdots$H-N-C in the both the cyclic tripeptides compared to that obtained from B3LYP/6-31G(d,p) level of theory. This might be due to accurate estimation of B97D functional for long range dispersion interaction comes from overlapping of π electrons of conjugated double bond at C-terminal end of the amino acids.

The linear tripeptides, **RRR** shows N-H$\cdots$O interaction with bond angle, $\angle$N-H$\cdots$O = 160.7° and distance H$\cdots$O = 2.31 Å (See Fig. S9) and **RRS** shows O-H$\cdots$N interaction with $\angle$O-H$\cdots$N = 170.2° and distance H$\cdots$N = 1.56 Å (See Fig. S10). Linearity and proximity of the bond supports larger stability of the peptide, **RRS** compared to **RRR** as shown in Fig. 3, which contradicts the result observed in gas phase.

In all, the data shows that kinetic favorability for formation of homochiral cyclic tripeptide over heterochiral cyclic tripeptide is reduced with the inclusion of solvent effect. We hope to further investigate this result in future studies using the explicit solvent phase model.

Conclusions

B3LYP and B97D functionals of density functional theory are used to gain inferences on homochiral versus heterochiral cyclic trimerization of 5-aminoethyl-3-methyl-2-imidazole carboxylic acid (**AEMIC**) in both the gas phase as well as solvent phase. Thermodynamically and kinetically homochiral cyclic tripeptide is favorable in gas phase. Even though, both the functionals, B3LYP and B97D show similar trends, the height of activation energy barriers is significantly reduced by the functional B97D compared to predicted by B3LYP. In solvent phase, the kinetic favorability of homochiral cyclic trimerization over heterochiral cyclic trimerization is reduced. The energetics of the peptides are substantiated by the structural parameters.

We suggest the use of B97D functional for the kind of systems studied in the present work.

Acknowledgments I thank Prof. Harjinder Singh, IIIT-Hyderabad and Prof. U. Deva Priyakumar, IIIT-Hyderabad for constant support and providing accessibility to computational facility. Also, I thank K L University, Vaddeswaram, Guntur for encouraging research activities.

References

1. Kohn W, Becke AD, Parr RG (1996) Density functional theory of electronic structure. J Phys Chem 100:12974–12980
2. Becke AD (1988) Density-functional exchange-energy approximation with correct asymptotic behavior. Phys Rev A 38:3098–3100
3. Grimme J (2006) Semiempirical GGA-type density functional constructed with a long-range dispersion correction. J Comput Chem 27:1787–1799
4. Riley KE, Pitonak MP, Jurecka P, Hobza P (2010) Stabilization and Structure calculations for noncovalent interactions in extended molecular systems based on wave function and density functional theories. Chem Rev 110:5023–5063
5. Jurecka P, Cerny J, Hobza P, Salahub DRJ (2007) Density functional theory augmented with an empirical dispersion term. Interaction energies and geometries of 80 noncovalent complexes compared with ab initio quantum mechanics calculations. Comput Chem 28:555–569
6. Holroyd LF, van Mourik T (2007) Insufficient description of dispersion in B3LYP and large basis set superposition errors in MP2 calculations can hide peptide conformers. Chem Phys Lett 442:42–46
7. Černy J, Jurečka P, Hobza P, Valdés HJ (2007) Resolution of identity density functional theory augmented with an empirical dispersion term (RI-DFT-D): A promising tool for studying isolated small peptides. Phys Chem A 111:1146–1154
8. Řeha D, Valdés H, Vondrášek J, Hobza P, Abu-Riziq AG, Crews B, de Vries MS (2005) Structure and IR spectrum of phenylalanyl-GlycylGlycine tripetide in the gas-Phase: IR/UV experiments, Ab Initio quantum chemical calculations, and molecular dynamic simulations. Chem -Eur J 11:6803–6817
9. Valdes H, Pluháčková K, Pitonák M, Řezáč J, Hobza P (2008) Benchmark database on isolated small peptides containing an aromatic side chain: comparison between wave function and density functional theory methods and empirical force field. Phys Chem Chem Phys 10:2747
10. Suresh Kumar NV, Singh H (2014) Density functional theory based study on cis-trans isomerism of the amide bond in homodimers of $\beta^{2,3}$- and β^3 - substituted homoproline. J Phys Chem A 118:2120–2137
11. Burns LA, Vázquez-Mayagoitia A, Sumpter BG, Sherrill CD (2011) Density-functional approaches to noncovalent interactions: A comparison of dispersion corrections (DFT-D), exchange-hole dipole moment (XDM) theory, and specialized functionals. J Chem Phys 134:084107
12. Zhao Y, Truhlar DG (2005) Benchmark databases for nonbonded interactions and their use to test density functional theory. J Chem Theory Comput 1:415–432
13. Suresh Kumar NV, Singh H, Kiran Kumar P, Chakraborty TK (2012) Preferential heterochiral cyclic trimerization of 5-(aminoethyl)-2-furancarboxylic acid (AEFC) driven by noncovalent interactions. J Mol Graph Model 38:13–25
14. Zhao Y, Truhlar DG (2008) The M06 suite of density functionals for main group thermochemistry, thermochemical kinetics, noncovalent interactions, excited states, and transition elements: two new functionals and systematic testing of four M06 - class functionals and 12 other functionals. Theor Chem Account 120:215–241
15. Tyndall JDA, Nall T, Fairlie DP (2005) Proteases universally recognize beta strands in their active sites. Chem Rev 105:973–999
16. Brea RJ, Amorn M, Castedo L, Granja JR (2005) Methyl-bolcked dimeric α, γ-peptide nanotube segments: formation of a peptide heterodimer through backbone-backbone interactions. Angew Chem Int Ed Engl 44:5710–5713
17. Kubik S, Goddard R (2001) Fine tuning of the cation affinity of artificial receptors based on cyclic peptides by intramolecular conformational control. Eur J Org Chem:311–322
18. Chakraborty TK, Tapadar S, Raju TV, Annapurna J, Singh H (2004) Cyclic trimers of chiral furan amino acids. Synlett 14:2484–2488
19. Christopher JW, Andrei KY (2011) Contemporary strategies for peptide macrocyclization. Nat Chem 3:509–524
20. Cavelier-Frontin F, Ppe G, Verducci J, Siri D, Jacquier R (1992) Prediction of the best linear precursor in the synthesis of cyclotetrapeptides by molecular mechanic calculations. J Am Chem Soc 114:8885–8890
21. Daidone I, Neuweiler H, Doose S, Sauer M, Smith JC (2010) Hydrogen-bond driven loop-closure kinetics in unfolded polypeptide chains. PLOS Comput Biol 6:276–288
22. Haberhauer G, Oeser T, Rominger F (2005) Molecular scaffold for the construction of three-armed and cage-like receptors. Chem Eur J 11:6718–6726
23. Marcus DH, Donald EC, David CL, Tim V, Eva Z, Geoffrey RH (2012) Avogadro: an advanced semantic chemical editor, visualization, and analysis platform. J Cheminformat 4:17
24. Hehre WJ, Radom L, Schleyer PVR, Pople JA (1986) Ab initio molecular orbital theory. Wiley-Inter Science, New York
25. Tomasi J, Persico M (1994) Molecular interactions in solution: an overview of methods based on continuous distributions of the solvent. Chem Rev 94:2027–2094
26. Bonaccorsi R, Palla P, Tomasi J (1984) Conformational energy of glycine in aqueous solutions and relative stability of the Zwitterionic and neutral forms. An Ab Initio Study. J Am Chem Soc 106:1945–1950
27. Mennucci B, Tomasi J, Cammi R, Cheeseman JR, Frisch MJ, Devlin FJ, Gabriel S, Stephens PJ (2002) Polarizable continuum model (PCM) calculations of solvent effects on optical rotations of chiral molecules. J Phys Chem A 106:6102
28. Tomasi J, Mennucci B, Cammi R (2005) Quantum mechanical continuum solvation models. Chem Rev 105:2999
29. Oie T, Loew GH, Burt SK, Binkley JS, MacElroy RD (1982) Quantum chemical studies of a model for peptide bond formation: formation of formamide and water from ammonia and formic acid. J Am Chem Soc 104:6169–6174
30. Jensen JH, Baldridge KK, Gordon MS (1992) Uncatalyzed peptide bond formation in the gas phase. J Phys Chem 96:8340
31. Krug JP, Popelier PLA, Bader RFW (1992) Theoretical study of neutral and of acid and base-promoted hydrolysis of formamide. J Phys Chem 96:7604–7616
32. Frisch MJ, et al. (2010) Gaussian, Inc., Wallingford, CT